Applied Thermal Engineering 127 (2017) 1326–1339

Contents lists available at ScienceDirect

Applied Thermal Engineering

journal homepage: www.elsevier.com/locate/apthermeng

Research Paper

Experimental investigation and modelling of thermal environment control of air distribution systems for chilled food manufacturing facilities

Demetris Parpas, Carlos Amaris *, Savvas A. Tassou

RCUK Centre for Sustainable Energy Use in Food Chains (CSEF), Institute of Energy Futures, Brunel University London, Uxbridge, Middlesex UB8 3PH, UK

HIGHLIGHTS

- Air distribution systems were investigated experimentally and numerically.
- The 3D models predicted well the air-temperature distribution.
- Different air temperature patterns were noted for each configuration.
- Fabric duct at a medium level achieved maximum temperature stratification.
- Ducts at medium level provided energy savings compared to the reference cases.

ARTICLE INFO

Article history:
Received 21 March 2017
Revised 20 August 2017
Accepted 28 August 2017
Available online 30 August 2017

Keywords:
Chilled food factories
CFD: Computational fluid dynamics
Air distribution systems
Refrigeration
Energy savings

ABSTRACT

Chilled food manufacturing facilities in the majority of cases have high ceilings to allow flexibility for the accommodation of different height equipment and manufacturing lines. The facilities are normally cooled by fan coil units located at ceiling level in a similar way to cold rooms, resulting in high velocities, uncomfortable environments for the workers and high energy consumption. To address these issues, this paper investigates the influence of different air distribution arrangements on air velocities and temperatures in a laboratory scale test facility and by means of a CFD model. The objective was to achieve low velocities and uniform temperatures at low level to achieve temperature stratification between floor and ceiling levels to reduce energy consumption. Experimental and CFD modelling results agreed that supplying air at medium level in the space through fabric ducts 'socks' could provide temperature stratification of the order of 7 °C between floor and ceiling level and energy savings in the region of 9% compared to ceiling mounted fabric ducts and 23% over non-ducted cooling coils mounted at ceiling level.

1. Introduction

The chilled food industry has shown significant growth in the last three decades. Based on data from the Chilled Food Association (CFA) the chilled food industry in the UK grew from £550 m in 1989 to £9755 m in 2012. In recent years, chilled food manufacturing in the UK has experienced annual increases of around 10% [1]. Refrigeration systems in the UK cold food chain are estimated to be responsible for 16,100 GWh energy use and 13.7 $MtCO_2e$ Greenhouse Gas Emissions. These represent approximately 28% of final energy use and 7% of GHG emissions of the whole food-chain [2].

Chilled food products have short shelf lives and need to be processed in facilities at temperatures in the range between +4 and +12 °C depending on the type of product, processing time and the desired minimum shelf time. Current food processing takes place in large spaces with high ceilings. In these spaces cooling is normally provided by ceiling mounted fan coil units drawing air from the space and discharging it back at high velocity directly through duct mounted diffusers. These systems employ the mixing cooling principle by which air is mixed in the entire room volume. This results in fairly uniform environments in terms of temperature and contaminant concentration but leads to energy wastage as all the air in the space volume is cooled to low temperature even though only the air at a low level, just above the food processing lines needs to be maintained at a low temperature for food safety and shelf life.

The air distribution patterns in large spaces can be obtained from experimental tests including flow visualisation studies and from modelling approaches. Studies to date have focused on air

* Corresponding author.
E-mail address: Carlos.amaris@outlook.com (C. Amaris).

http://dx.doi.org/10.1016/j.applthermaleng.2017.08.134
1359-4311/

distribution in large spaces in commercial buildings for ventilation and air conditioning applications to provide thermal comfort for the occupants and reduce energy consumption, and in cold rooms where the priorities are to maximise the holding volume and provide uniform temperatures in the space. Very little work has been reported in the literature on air distribution in chilled food factories where the objective is to maintain the temperature at low levels for food safety and quality but also reduce thermal discomfort for the occupants in the space.

Regarding experimental studies dealing with air distributions systems, Rees and Haves [3] studied the air flow mixing and overall temperature gradient in a room with displacement ventilation and chilled ceiling for office environments. The authors found that significant air mixing reduces temperature gradients in the upper part of the room. Cheng et al. [4] analysed the effect of different locations for the supply and return grilles on thermal comfort and energy savings. The authors showed that temperature stratification in the space can provide both energy savings and thermal comfort for the occupants. Lin and Tsai [5] studied the effect of supply diffuser position and supply air flow rate on the thermal environment of an indoor space. The authors reported that for a given diffuser, the temperature gradient in the space reduces as the supply air flow increases due to greater mixing between the room and supply air.

Menwhile, Jurelionis et al. [6] investigated the impact of the air supply method on the ventilation efficiency in a test chamber. In this investigation, the aerosol particle dispersion with different air distribution methods was analysed. Results showed that the one-way mixing ventilation ceiling diffuser with low flow rate was more efficient in terms of ventilation in comparison with the four-way mixing and high air exchange rates. It was also concluded that the displacement air distribution method was less efficient than the mixing ventilation in terms of air removal. Rhee et al. [7] evaluated the performance of an active chilled beam system in terms of uniformity for an indoor thermal environment in a full-scale test bed. The authors reported acceptable thermal uniformity with the active chilled beam system even at low air flow rates.

Airflow modelling techniques have been developed over the last 30 years to provide a better understanding of air flow patterns and temperature distribution in large spaces including cold rooms. Smale et al. [8] reviewed CFD modelling applications for the prediction of airflow in refrigerated food storage applications. It was reported that the k-ε turbulence model was not accurate enough to be used in many refrigerated food storage applications and the RSM (Reynolds Stress Model) provided higher degrees of accuracy. Ambaw et al. [9] reviewed the application of CFD for the modelling of post-harvest refrigeration processes. The finite volume method with the upwind differencing scheme was identified as the most common solution method. In addition, it was reported that the Reynolds Stress Model (RSM) provides more accurate predictions compared to the conventional k-ε model but the k-ε model is more commonly used due to its lower computational requirements.

Laguerre et al. [10], in order to avoid the computational time of a CFD model, created a simplified model using the knowledge obtained from experimental measurements. The model was separated into zones and heat balance equations for each zone were developed. The simplified model was found to predict the product cooling rate and the final product temperature at different positions in the cold room quite well [10,11].

For its part, Delele et al. [12] developed a multi-scale CFD model using 4 different two-equation eddy-viscosity turbulence models to predict air velocity, temperature and humidity distribution in a loaded cold room. Results showed that the Standard k-ω /SST k-ω models provided better air velocity prediction accuracies when compared to experimental data. Delele et al. [13] also developed a 3-D model in CFD in order to predict air flow and heat transfer characteristics of a horticultural produce packaging system. The air flow in the space was solved using the Reynolds averaged Navier Stroke equations (RANS). The standard k-ε, RNG k-ε and standard k-ω two equation turbulence models were considered and the SST k-ω was found to produce the most accurate predictions of air pressure drop and produce temperature when compared to experimental data. In addition, CFD numerical studies from the literature show that prediction of air velocity, temperature distribution and mean age of the air in different food refrigerated spaces can be obtained in good agreement with experimental data [14,15,16,17,18].

Moreover, Pasut et al. [19] simulated underfloor air distribution via fabric ducts and rigid ducts. The authors mainly focused on the analysis of the discharge air temperature and flow through the diffusers. The k–e turbulence model was employed in the CFD model. The authors also conducted experiments in a full-scale underfloor plenum in order to validate the developed CFD models. Recently, Fathollahzadeh et al. [20] studied the effect of using two types of inlet diffusers (direct and swirl) with combined and separate return and exhaust air vents on the thermal comfort, indoor air quality and energy consumption in an indoor environment. Main results showed that the energy consumption of the system decreased by reducing the height of return air vent from ceiling to floor height. In general, numerical studies involving stratified air temperature are available for the performance analysis of underfloor air distribution systems [19–21], or for the optimization of thermal comfort and energy savings [22,23]. Lastly, Tassou et. al. [24] provided a review of modelling approaches of chilled spaces in the cold food chain.

According to the literature, there are not studies evidencing air-temperature distribution issues in chilled food processing facilities and its effect on the refrigeration plant energy consumption. Therefore, this paper describes CFD modelling and experimental investigations into air velocity and temperature distribution in an experimental test facility designed to represent chilled food processing environments. The objective was to investigate ways of providing low air temperatures and velocities at a low level to satisfy food manufacturing regulations whilst reducing energy consumption of the refrigeration plant.

2. Procedure

The initial stage of this research was focused on understanding the air flow and temperature variation in existing chilled food facilities using measurements and CFD modelling [24,25]. The research reported in this paper deals with the experimental investigation and CFD modelling of different air distribution arrangements to achieve temperature stratification in the space and reduce energy consumption.

2.1. Experimental facility

The experimental test rig was established using an environmental chamber constructed with insulated cold room panels. The chamber dimensions are 2.9 m (H) × 6.6 m (L) × 3.5 m (W). Cooling in the chamber was provided by an evaporator coil served by an R404a condensing unit situated outside the test rig in the ambient air. A schematic diagram of the layout of the test rig is shown in Fig. 1. For the initial experiments, two air distribution methods were tested.

(i) Evaporator coil without any ducting as shown in Fig. 2a.
(ii) Air distribution using fabric ducts (tests were performed with a duct of 0.4 m in diameter and 4.0 m in length installed at ceiling level as illustrated in Fig. 2b.

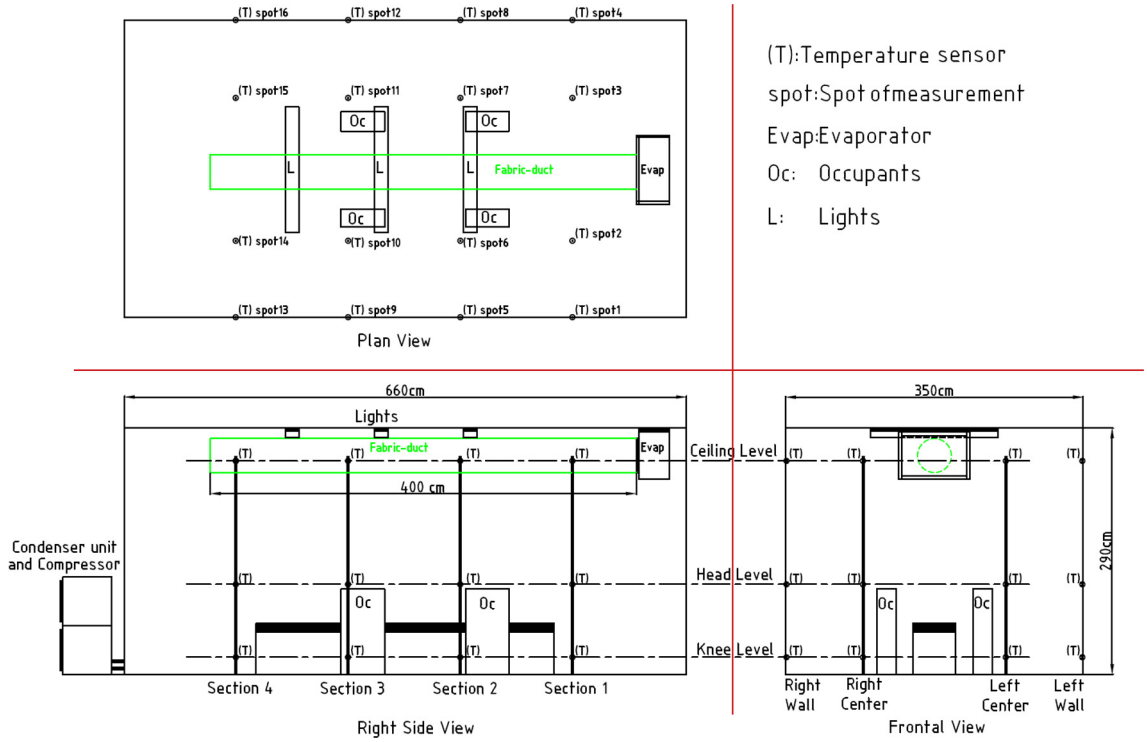

Fig. 1. Outline of the experimental test facility with air distribution via fabric duct at ceiling level, reference case.

Fig. 2. Experimental test facility: [a] air distribution via plain evaporator coil and [b] air distribution via a round fabric duct.

The first configuration is used in a large number of chilled food manufacturing facilities. In the case of the air distribution via fabric duct, it appears as an attractive option due to its practical design, reduced acquisition and maintenance cost and homogeneous air flow if compared to metal-based air distribution systems. The fabric duct that was used in the 2nd experimental set-up was fabricated with the 'KE - Low Impulse textile duct fabric' of Ke-fibertec [26]. Air temperature measurements in the chamber, using T-type thermocouples, were taken at 4 sections along the length of the chamber (see Fig. 1) and 4 sections along the width of the chamber (Right-wall, Right-centre, Left-centre and Left-wall) and at three heights, knee level, head level and ceiling level. In total, 48 temperature sensors were installed. The thermal load from occupants (OC) was simulated by 4 rectangular boxes of 1.6 m^2 surface area each wrapped with trace heater elements, 150 W each. The measured temperature at the top of the occupants was on average of 14 °C. Air velocity measurements were also taken close to the position of each temperature sensor using an air flow meter TSI TA465-P with a thermo-anemometer probe 966 [27].

The electrical power consumption of the refrigeration system was recorded by a portable power meter Fluke 435 Series II [28]. A variable speed controller was also used to control the supply air. In addition, four data scan flow modules 7020 used for the temperature [29]. The logging interval of the data was set to 10 s. The time for each test was 17 h.

Table 1 presents the measurement uncertainties of the used sensors. The air temperature in the test chamber was controlled using a temperature controller with the thermostat located on the evaporator air suction side and set to 9.7 °C.

2.2. CFD model details

The dimensions of the scaled model volume are those of the experimental test room. The HVAC system consisted of a single evaporator coil circulating the air. As in the case of many existing processing facilities, the evaporator is operated with 100% recirculated air. The evaporator is controlled by a thermostat with 9.7 °C air-of set point temperature. The steady state 3-D CFD model was solved using the commercial ANSYS FLUENT® package [30].

Table 1
Measurement uncertainties of the sensors.

	Operating range	Uncertainty
Sensors		
Thermocouples with TC adapter, (°C)	−50–400	±0.5 °C
Thermoanemometer - Air flow meter, ($m.s^{-1}$)	0–50	±3.0%
Energy logger - Power consumption, (Arms)	1–400	±0.5%

2.2.1. Boundary conditions

The air flow supply and return from the evaporator were initially set at 2825 m^3 hr^{-1}. The air supply from the supply and return air sections at the coil boundary conditions were defined as mass flow inlets and outlets, respectively. The air supply temperature was set at 7 °C. The occupancy density of the investigated processing area was set at 4 occupants taking into account the scaled model area. Each occupant was defined as a rectangular box with a 1.57 m^2 surface area (1.2 m height) with a sensible thermal load of 150 W. The lighting heat load was set at 30 Wm^{-2} floor area. Other heat sources into the processing area were neglected. The thermal boundary conditions of the surrounding walls were approached taking into account the thermal resistances (Eq. (1)) and heat flow (Eq. (2)) from the exterior to the interior of the chamber, and considering an outdoor temperature of 20 °C. The wall thickness was 0.1 m while the thermal conductivity of the wall was 0.023 $W{\cdot}m^{-1}{\cdot}K^{-1}$. The exterior and interior wall surfaces resistances were 0.13 $m^2{\cdot}K{\cdot}W^{-1}$ and 0.04 $m^2{\cdot}K{\cdot}W^{-1}$ respectively.

$$Ui = \frac{1}{(Rsi + R1 + Rse)}\left(\frac{W}{m^2}K\right) \tag{1}$$

$$q = Ui \times \Delta T\left(\frac{W}{m^2}\right) \tag{2}$$

2.2.2. CFD simulation solution procedure

The model was solved with the pressure based solution algorithm, second order upwind energy and momentum discretisation, 'Body-Force' weighted pressure discretisation, and SIMPLE pressure-velocity coupling. The air inside the processing area was considered to be compressible and the density was allowed to vary according to the ideal gas law to account for buoyancy effects. Other thermal properties (such as specific heat, thermal conductivity and viscosity) were maintained constant. Even though, according to the literature, the Reynolds Stress Model (RSM) provides more accurate predictions compared to the conventional k-ε models, the SST-k-ω turbulence model was applied in this simulation since it was found to predict measured data with good accuracy and a reasonable computational time. The SST k-ω model has also been pointed out in open literature as a more accurate model in comparison to the others k-ε and k- ω models [8,9,19,21,31].

The SST-k-ω turbulence model is a two-equation eddy-viscosity model (Eqs. (3) and (4)) which was developed by Menter [32] to effectively blend the robust and accurate formulation of the model in the near-wall region. In general, two-equation turbulence models allow the determination of the turbulent length and the time scale by solving two separate transport equations. The main difference from the turbulent viscosity definition of the standard k-ω turbulence model is that the modelling constants take into account the transport of the turbulent shear stress. The SST-k-ω turbulence model combines the usage of the k-ω formulas for the inner parts of the boundary layers and the usage of the SST formulation in the free-stream. As a result, the SST-k-ω turbulence model can be used as a Low-Re turbulence model without any extra damping functions and by switching to the k-ε behavior, the common k-ω problem where the model is too sensitive to the inlet free-stream turbulence properties is avoided. The SST-k-ω turbulence model is more accurate and reliable for a wider class of flows than the standard k-ω model.

The following transport equations define the SST-k-ω turbulence model.

$$\frac{\partial}{\partial t}(\rho k) + \frac{\partial}{\partial x_i}(\rho k u_i) = \frac{\partial}{\partial x_j}\left\{\Gamma_k \frac{\partial k}{\partial x_j}\right\} + \widetilde{G_k} - Y_k + S_k \tag{3}$$

$$\frac{\partial}{\partial t}(\rho \omega) + \frac{\partial}{\partial x_j}(\rho \omega u_j) = \frac{\partial}{\partial x_j}\left\{\Gamma_\omega \frac{\partial \omega}{\partial x_j}\right\} + G_\omega - Y_\omega + D_\omega + S_\omega \tag{4}$$

In Eq. (3), $\widetilde{G_k}$ represents the generation of turbulence kinetic energy due to mean velocity gradients. In Eq. (4), G_ω represents the generation of ω which is calculated in the same way as the standard k-ω turbulence model. Γ_k and Γ_ω represent the effective diffusivity of k and ω respectively, and Y_k and Y_ω represent the dissipation of k and ω due to turbulence. D_ω is the cross-diffusion term, and S_k and S_ω are user-defined source terms. More details of the turbulence model can be found in Ref. [30,32].

2.2.3. Mesh generation

The computational domain was discretized with an automatic mesh method, with mainly tetrahedral cells (with hexahedral cells in the boundary layer). The mesh density was gradually refined near the building wall, the fabric duct and other surfaces in the space. The final mesh size consisted of 9.4 million elements for the case of the plain evaporator and 9.6 million elements for the case of fabric duct. The element dimensions for both cases varied between 0.02 AND 0.06 m (0.02 for lighting, occupants and sock. 0.04 for evaporator outlet. 0.06 for productions evaporator body and walls). The finer mesh sizes were located near the wall surfaces, where 4 inflation layers were also employed to capture the effects of the boundary layer. The final model mesh was generated following a mesh independency study. The simulation time for each steady-state case was 8 h, with an average of 3000 iterations, on a 2.5 GHz, 64 GB RAM, Intel Xeon Processor (2 processors) with 48 parallel threads. Fig. 3 shows the developed CFD models for the two investigated air distribution solutions.

Fig. 4 shows an example of the mesh independency study implemented in order to conclude to a mesh independent solution. The convergence criteria for the independency study were set to

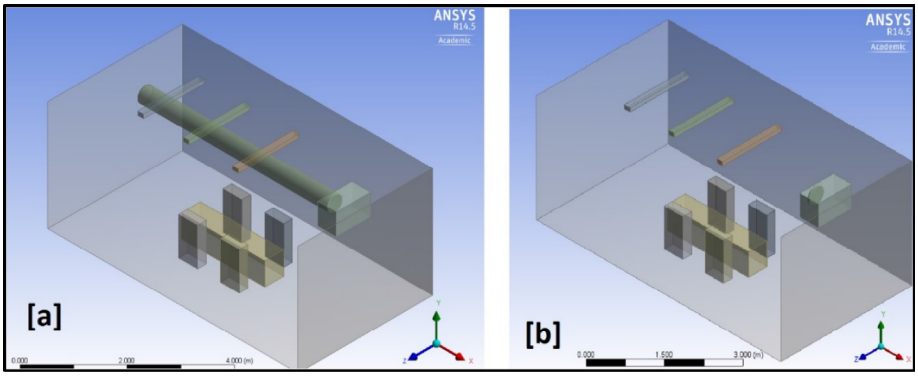

Fig. 3. 3-D models (a) with Fabric duct and (b) Plain evaporator.

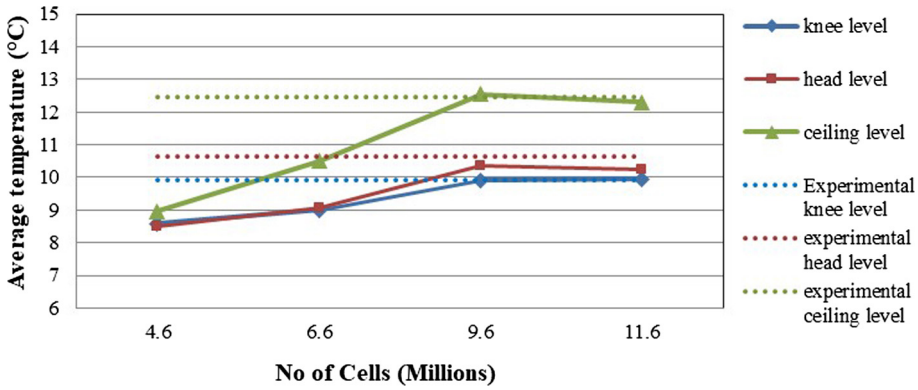

Fig. 4. Mesh independency study. Fabric duct at ceiling level.

reach at least a 10–5 residual error for continuity and an average temperature tolerance of ±0.5 °C. The 3 values of interest were the average temperatures at knee, head and ceiling level height. The initial mesh size was at 4.6 million cells and the solution convergence criteria were met at 3000 iterations. Fig. 4 shows that a solution was reached independently of the mesh resolution at 9.6 million cells. In addition, comparing with experimental values the mesh with 9.6 million cells size provides a good prediction.

3. Results and discussion

This section discusses the results of the experimental measurements and CFD modelling of the thermal environment arising from the air distribution system via plain evaporator coil and fabric duct. Then the analysis of an air distribution system is presented that is located at a medium level as an alternative configuration. Finally, the energy consumptions of the refrigeration system with the different air distribution configurations are compared.

3.1. Air distribution via plain evaporator coil

This sub-section presents the results of the experimental measurements and CFD modelling of the thermal environment from the air distribution system via plain evaporator coil installed at ceiling level as shown in Fig. 2a.

3.1.1. Experimental test

Fig. 5a shows the temperature profiles from measurements in the test chamber with air distribution via plain evaporator coil installed at ceiling level. The evaporator fan velocity was set at 100 % which corresponds to the volumetric flow rate of 2825 $m^3\ h^{-1}$. Temperature values correspond to the average values measured at each position. The average temperatures measured at knee, head and ceiling level were 7.8 °C, 7.6 °C and 7.2 °C with a ±0.5 °C variation in each point of measurement, respectively. It can be noted that the air temperatures were fairly uniform in the space with no temperature stratification. In addition, it is observed that higher temperatures were obtained at the knee and head level which may be the result of the heat gains from the occupants.

Air velocities in the space are shown in Fig. 5b. They varied between 0.2 and 2.2 $m\ s^{-1}$ with highest values recorded at ceiling level from the direct air discharge of the non-ducted cooling coil. The average velocities across all measurement points for the knee, head and ceiling level were 0.45 $m{\cdot}s^{-1}$, 0.37 $m{\cdot}s^{-1}$ and 0.82 $m{\cdot}s^{-1}$ respectively. At knee and head level, the velocity at some measurement points was as high as 1.0 $m{\cdot}s^{-1}$ which may create an uncomfortable environment for workers around the production zone.

Based on the experimental data collected, it can be confirmed that the air distribution system via non-ducted coil is effective to maintain the required temperature conditions around the production lines, which is the main requirement in order to conserve food with a high quality during its processing. On the other hand, it can also be observed that the whole space is cooled down at almost the same temperature. In chilled food processing facilities where large spaces are required, this would imply high energy consumptions from the refrigeration units given the poor temperature stratification observed in the whole space of the facility.

3.1.2. CFD modelling

Fig. 6a shows the air temperature distribution in the space with a supply air temperature from the evaporator at 7 °C. The temperature in the bulk of the space varied between of 7.0 °C and 8.0 °C considering the same measurement points of the experimental test. As seen in Fig. 5a. temperature modelling results showed insignificant temperature variations around the space. In addition, it can be observed that higher temperatures were found close to the occupants due to the heat gains from those. This agreed with the data collected from the measurements which also showed the highest temperatures at a low level, mainly around the occupants.

Furthermore, Fig. 6b shows the velocity distribution at 4 cross sections along the space from modelling the air distribution system via plain evaporator at ceiling level. Modelled air flow velocities in the space were found to be significantly high ranging from 0.02 to 3.0 $m{\cdot}s^{-1}$. As also noted experimentally, it is observed that the highest air flows were found at ceiling level due to the direct air discharge from coil employing a small air flow area. In addition, the CFD model results show some air-draft at knee and head level which can lead to excessive discomfort for the occupants according to the BS EN ISO 7730:2005 [33].

It can also be observed that the air flow patterns over the space are not homogeneous and that air velocities are also relatively high close to the front wall. The air flows along the ceiling to the front wall, and then it flows down next to the wall until it reaches the floor. Then, recirculation takes place in an area between floor level and ceiling level. From Fig. 6b it can also be observed that the air displacement around the space is mainly influenced by the high air flow velocity from the coil rather than buoyancy effects due to heat gains from the workers and equipment.

Based on the CFD modelling results, it can be highlighted that this type of air distribution method tends to cool-down uniformly the whole volume of the space at very high and nonhomogeneous air flow velocities leading to an excessive discomfort and non-energy efficient system. In addition, Fig. 7 presents the average

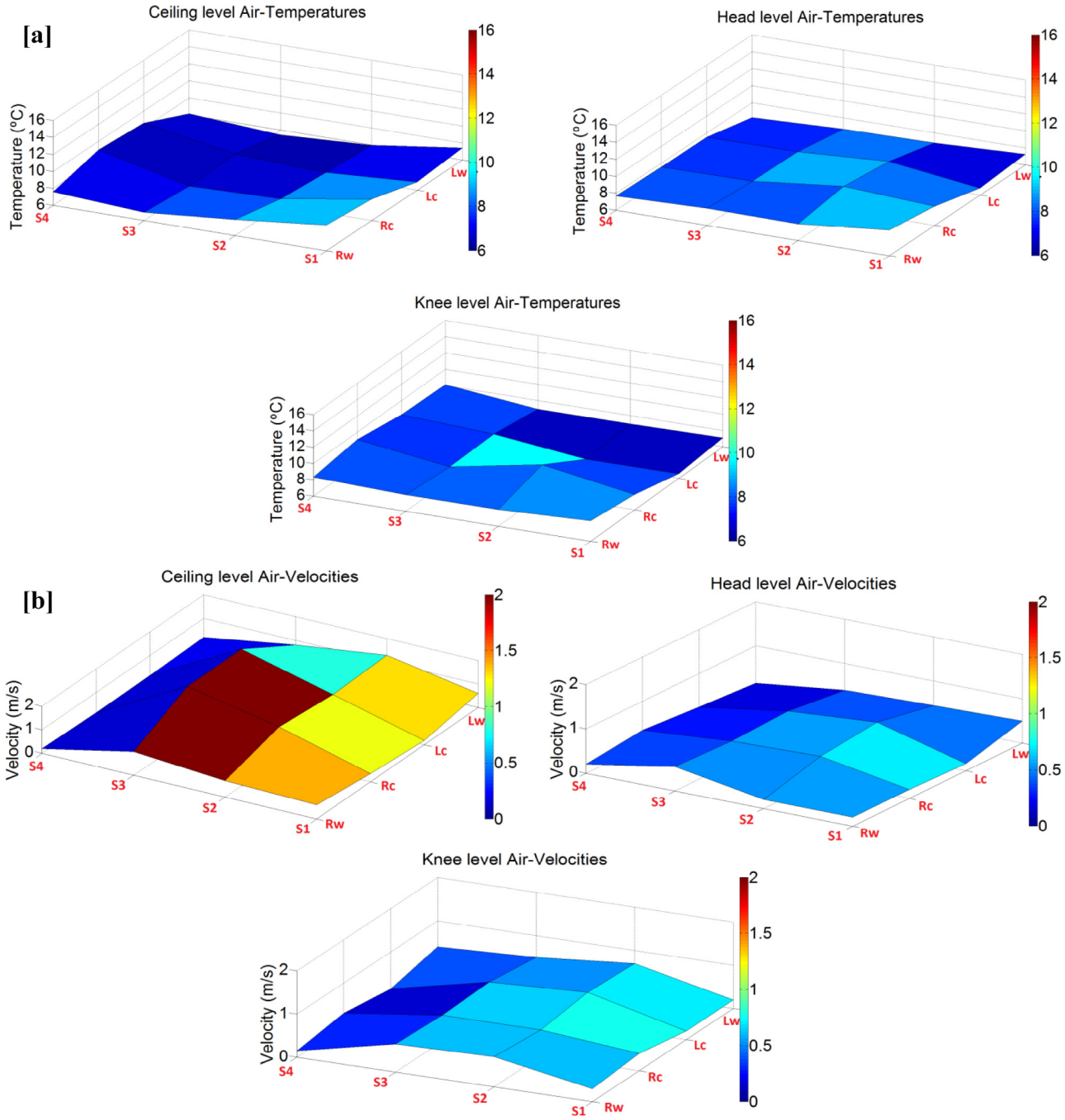

Fig. 5. Measurements at different heights; Knee Level, Head Level and Ceiling Level. [a] Temperature profiles and [b] Velocity profiles.

temperature and velocities data collected including a measurement uncertainty of ±0.1 $m \cdot s^{-1}$ and the modelling results. In general, the model shows a good level of prediction for the air temperature and velocity trend and distribution achieved in the space. From the results, the average absolute error across all test points in the space was found to be 0.73 °C and 0.6 $m \cdot s^{-1}$.

3.2. Air distribution via fabric duct at ceiling level

This sub-section presents the experimental measurements and CFD modelling of the thermal environment from the air distribution system via a round fabric duct installed at ceiling level as shown in Fig. 2b.

3.2.1. Experimental test

Fig. 8a shows the temperature profiles from measurements in the test chamber with air distribution via fabric duct at ceiling level. The evaporator fan velocity was set at 100 % which corresponds to the volumetric flow rate of 2825 $m^3\ h^{-1}$. Temperature values in Fig. 8a correspond to the average values measured at each position. The average temperature values measured at knee, head and ceiling level were 9.9 °C, 10.6 °C and 12.4 °C with a ±0.5 °C variation in each point of measurement, respectively.

According to the data recorded, some temperature stratification was obtained with the lowest temperatures measured at knee level and highest at ceiling level. It was also observed that the temperature stratification between the three measuring heights followed an apparent steady distribution pattern. Furthermore, it can also be

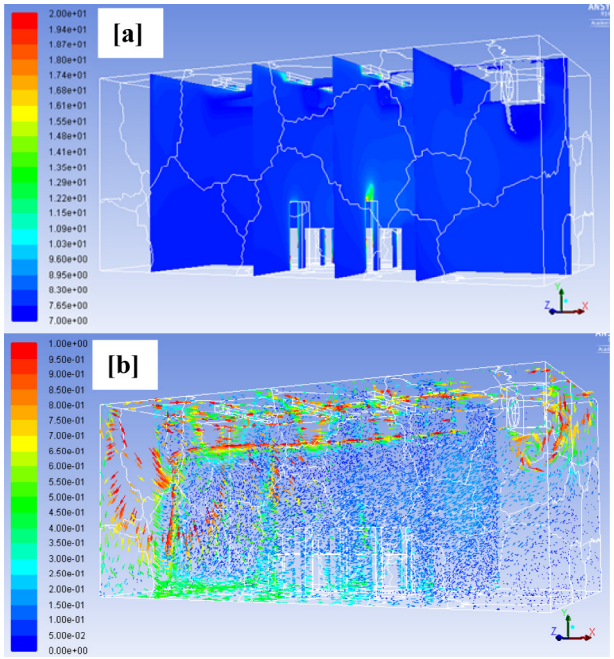

Fig. 6. CFD Simulation of [a] air temperature in the space (°C) and [b] air velocity ($m{\cdot}s^{-1}$).

noted in Fig. 8a that the highest temperatures were obtained close to the walls at ceiling level which may be due to the fact that the air around those sections was not directly cooled by the air flowing from the fabric duct. In the case of the central section, the air temperature may be influenced by the heat gains from the lightings. In addition, it was also observed that the heat gains from the occupants influenced the temperature measurements of the sensors located around the centre of the facility and that the lowest temperatures were basically obtained close to the walls at knee level.

Regarding the air velocities shown in Fig. 8b, measured values varied between 0.02 and 0.25 m s^{-1} with highest values recorded at knee level. In this case, the highest velocity values found at knee level may be caused by return and supply effect of the cooling coil unit which provided recirculation of air in the space. Maximum air velocity close to the fabric duct was found to be 0.17 m s^{-1}. In general, it can be said that the variation of air velocities was within the range expected in air conditioned spaces and should not create drafts in the space.

Comparing the air flow velocities obtained from the air distribution system via the non-ducted coil and fabric ducts it can be highlighted that the fabric duct provided much lower air flow velocities. This is beneficial to achieve some temperature stratification mainly around those space adjacent to the walls in comparison to the case of the non-ducted coil.

3.2.2. CFD modelling

This subsection presents the results regarding the CFD modelling of the experimental facility using fabric ducts as an air distribution method.

Fig. 9a shows the air temperature distribution in the space with a supply air temperature from the fabric duct at 7 °C. The temperature in the bulk of the space varied between of 8.9 °C and 13.4 °C considering the same measurement points of the experimental test. This means that, as seen from the experimental results, some temperature stratification was obtained with lowest temperatures measured at knee level and highest at ceiling level.

Moreover, Fig. 9a clearly shows that space below the fabric ducts and above head level present even lower temperatures that those between head level and knee level due to the low temperature of the air supplied directly from the fabric ducts. The aforementioned confirms the influenced of the heat gains from

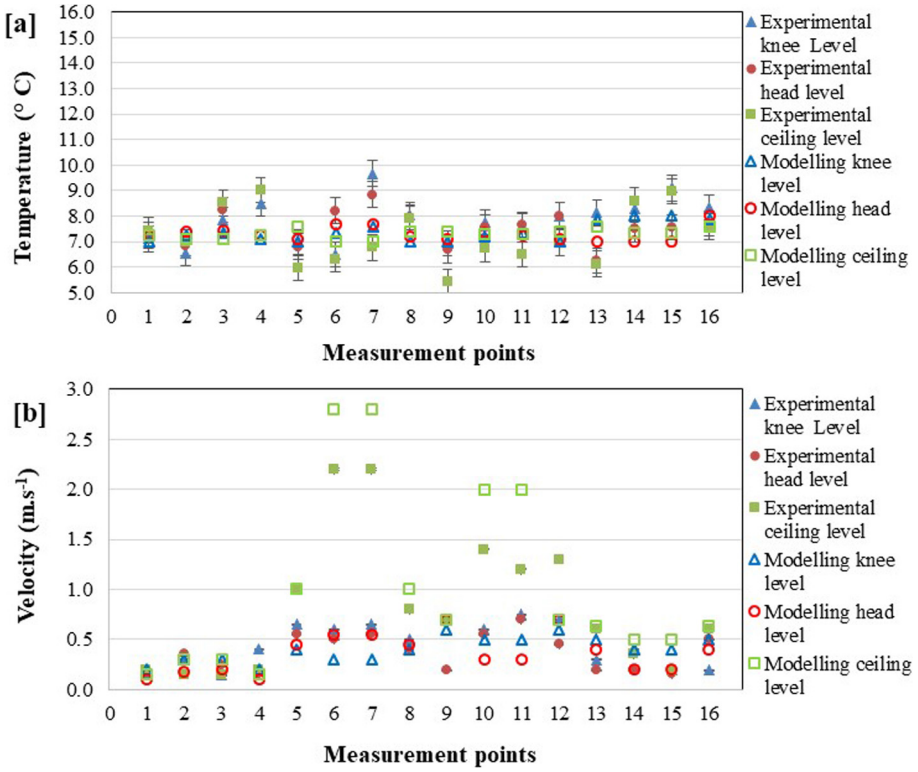

Fig. 7. Experimental and CFD modelling results comparison for [a] air temperature and [b] air velocity.

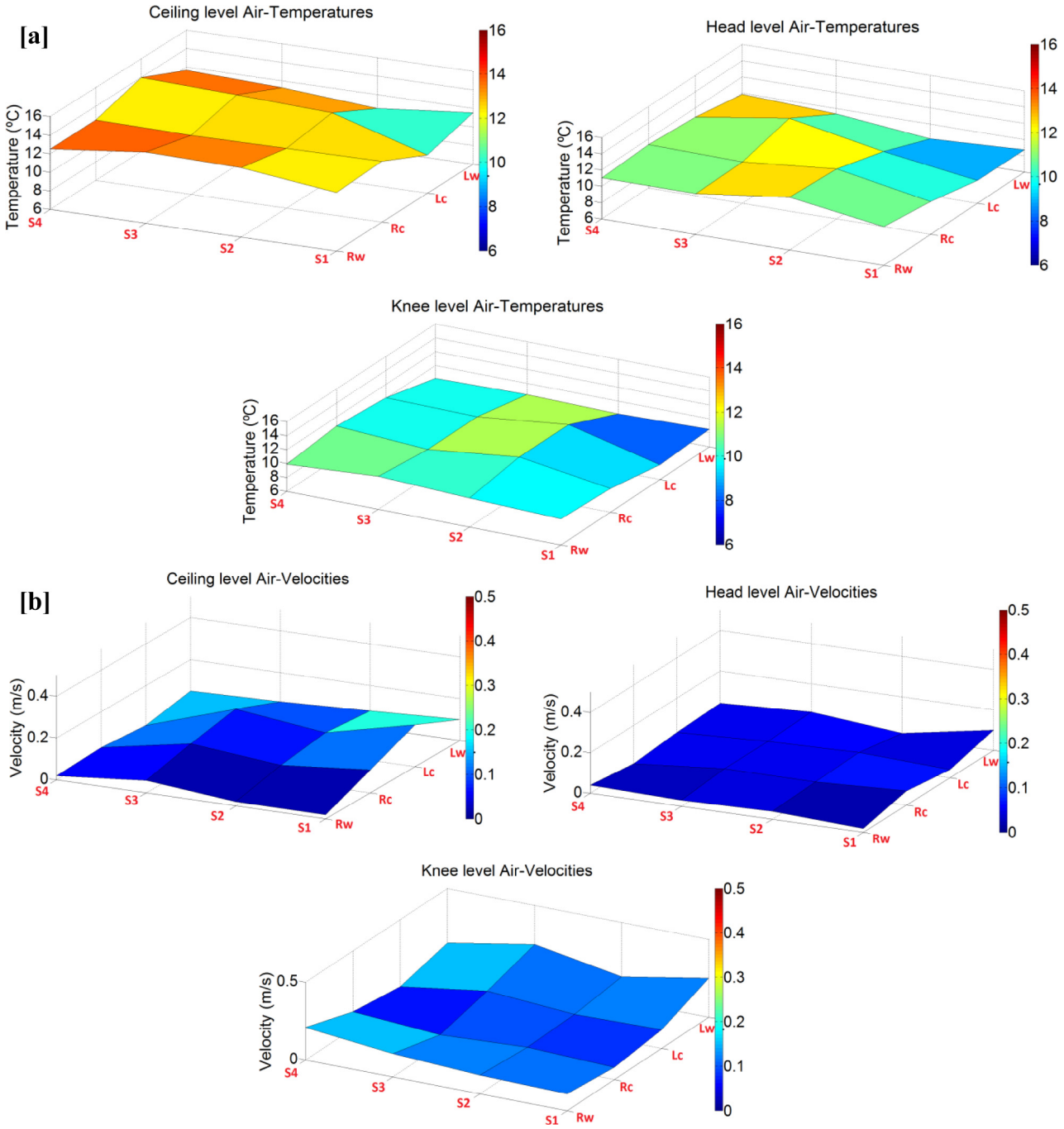

Fig. 8. Measurements at different heights; Knee Level, Head Level and Ceiling Level. [a] Temperature profiles and [b] Velocity profiles.

occupants and lightings on the air temperature values obtained experimentally around this area at knee and ceiling level.

Fig. 9b shows the velocity distribution at 4 cross sections along the space from modelling the air distribution system via fabric duct at ceiling level. Modelled air flow velocities in the space were found to be very low and ranging from 0.01 to 0.3 $m \cdot s^{-1}$. It is observed that the highest air flows were found close to the air return section. Some air movement was also noted directly under the fabric duct and above the occupants, the latter one occurring due to the buoyancy effects.

Fig. 10 presents the average temperature and velocity data collected, including a measurement uncertainty of ±0.05 $m \cdot s^{-1}$ and the modelling results. In general, the model shows a good level of prediction for the air temperature distribution and velocity trend achieved in the space. From the results, the average absolute error across all test points in the space was found to be 0.95 °C and 0.1 $m \cdot s^{-1}$.

In general terms, the accuracy of predicted air temperatures compared with experimental data are in a good agreement. Tables 2 and 3 show a comparison of the average temperature and velocities cross all the measuring points at different measuring heights between the predicted and measured values. From those it can be seen that the average values between the experimental and modelled values at different heights follow the same pattern.

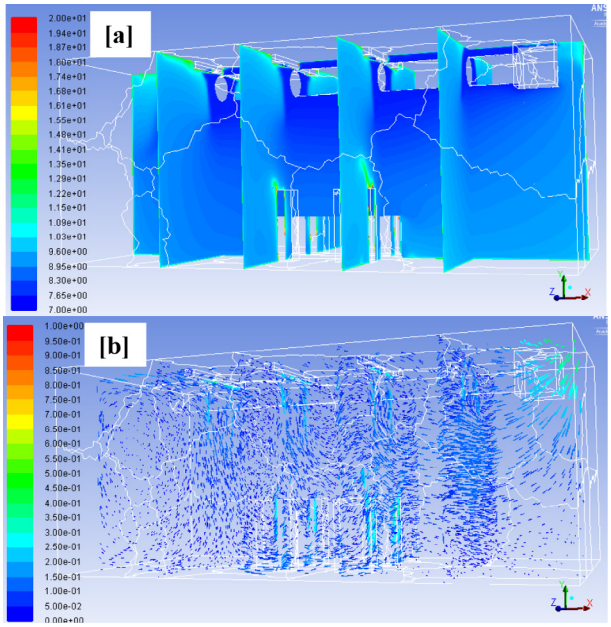

Fig. 9. CFD Simulation results of [a] air temperature in the space and [b] air velocity ($m{\cdot}s^{-1}$).

From the above results, it can be concluded that the fabric duct delivered a better environment in the space in terms of air velocity uniformity at the level of the production area. This was mainly due to the lower air velocities in the space obtained with the fabric duct air distribution method. Therefore, there was a clear influence of the air flow velocity on the temperature stratification obtained in the space. In addition, the fabric duct resulted in average air temperature stratification in the space of the order of 2.5 °C.

Table 2
Plain evaporator coil: CFD predicted values vs. measured values overview.

Experimental facility: Plain evaporator coil at Ceiling level			
	Average temperatures (°C)		
	Knee level	Head level	Ceiling level
Predicted	7.4	7.3	7.3
Measured	7.8	7.6	7.2
	Average Velocities ($m.s^{-1}$)		
	Knee level	Head level	Ceiling level
Predicted	0.400	0.360	1.010
Measured	0.450	0.380	0.820

Table 3
Fabric duct at Ceiling level: CFD predicted values vs. measured values overview.

Experimental facility: Fabric duct at Ceiling level			
	Average temperatures (°C)		
	Knee level	Head level	Ceiling level
Predicted	9.9	10.3	12.5
Measured	9.9	10.6	12.4
	Average Velocities ($m{\cdot}s^{-1}$)		
	Knee level	Head level	Ceiling level
Predicted	0.030	0.060	0.11
Measured	0.070	0.044	0.13

3.3. Air distribution via fabric ducts at a medium level

Most chilled food factories operate 7 days per week, 24 h per day with short breaks mainly for cleaning and shift changes. Any modifications or changes to the current air distribution systems need to be implemented during those short breaks in order to avoid any disruption to food production. In a previous study, the air flow and temperature from different alternative systems

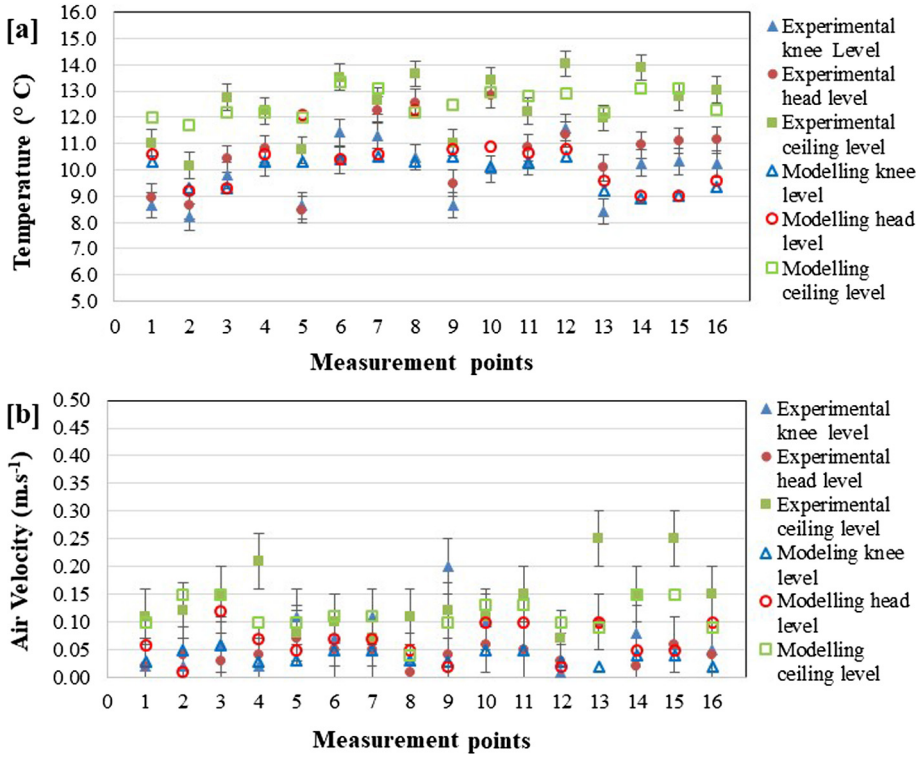

Fig. 10. Experimental and CFD modelling results comparison for [a] air temperature and [b] air velocity.

(including air distribution via displacement ventilation with diffusers supply at a low level and a metal based-slot diffuser at a medium level) were simulated [34]. However, these systems were not suitable for the application under study due to the fact that they were not able to provide homogeneous and low air flow around the space. Therefore, an improved air distribution method needs to provide homogenous air flow throughout the occupied zone and to be easily adaptable to the cooling systems currently installed to an existing chilled food facility.

Taking into account these constraints, the air distribution system via round (circular) fabric duct located at a medium level was selected for further modelling and experimental investigation to establish their effectiveness in providing temperature stratification leading to energy efficiency. Additionally, an air distribution system via D-shape duct or half duct was also analysed with the same purpose. Both systems can be easily retrofitted to evaporator coils without ducted air distribution systems placed at ceiling level. The easy implementation of both systems in existing chilled food facilities is, therefore, a favourable aspect which contributed in their selection.

3.3.1. CFD modelling and experimental verification

This section presents the results from the CFD modelling and experimental study of the air temperature and flows distribution via round (circular) fabric duct and D-shape duct located at a medium level.

Both ducts measured 0.40 m diameter and 4.0 m length. The only difference to the reference case was that the centre line of the ducts was 1.15 m below ceiling level compared to 0.25 m for the reference case.

Figs. 11 and 12 show the air temperature and flow distribution using fabric ducts installed at a medium level. From Fig. 11a it can be observed that the air temperature distribution from the round fabric duct was homogenous around the occupied zone at the different heights with no significant difference between the head and ceiling level. With a supply temperature of 7 °C from the fabric duct, the temperature in the bulk of the space varied between 8.0 °C and 15 °C, with an average temperature at production height of 8.0 °C. Temperature stratification was observed, with the lower temperatures presented at the occupied space. The highest temperatures where identified at the ceiling level, as expected. Moreover, Fig. 11b shows that when the D-shape fabric duct at a medium level was modelled, the temperature in the bulk of the space varied between 7 °C and 14.0 °C, with an average temperature at production height of 7.1 °C. Interestingly, the temperature gradients were more pronounced between the head level and the ceiling level, keeping the space below the head level at a lower temperature.

In addition, Fig. 12a and b show that the air distribution system via fabric ducts at a medium level provided homogeneous flow patterns along the space with very low air velocities (between 0.02 and 0.3 $m \cdot s^{-1}$) and maximum air velocities of 0.3 $m \cdot s^{-1}$ close to the fabric duct in the case of the D-shape fabric duct.

Base on the CFD modelling results, the fabric ducts located at a medium height level seem to be an adequate configuration for air distribution in large spaces as those in chilled food processing facilities. According to the CFD model results, the fabric ducts could provide a remarkable level of temperature stratification and air flow homogeneity over the production zone, together with an easy implementation in an actual factory situation. It allows discharging a high cooled air volume though the whole surface of the fabric duct at low and uniform air velocities.

Following the CFD modelling results, fabric ducts at a medium level were also tested at the laboratory for verification purposes. Fig. 13a shows the experimental set-up for the round fabric duct. Additionally, Fig. 13b shows a D-shape fabric duct design installed at a medium level.

Fig. 14a and b show the average temperature profiles in the experimental test facility for the round and D-shape ducts, respectively, both installed at a medium level. Temperature values correspond to the average values measured at each position with a ±0.5 °C variation in each point of measurement. For the round fabric duct, average temperature values measured at knee, head and ceiling level were 9.8 °C, 10.7 °C and 15.2 °C respectively. On the other hand, the implementation of the D-shape duct resulted in average temperature values measured at knee, head and ceiling level of 9.3 °C, 10.5 °C and 14.3 °C respectively. In both cases, it can be seen that a significant temperature gradient was established between the floor and ceiling level (of the order of 5 °C) with colder air flows concentrated at a low level in the space. In addition, most

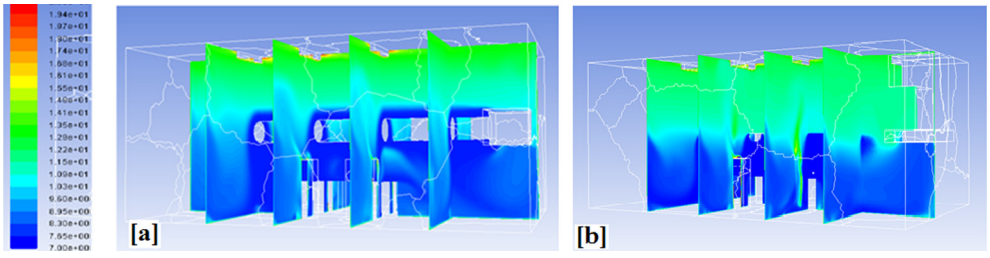

Fig. 11. 3-D CFD models air temperature profiles via [a] fabric duct at a medium level and [b] D-shape fabric duct at a medium level.

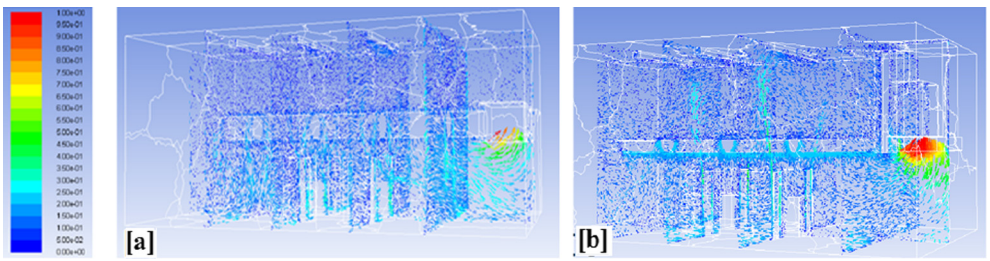

Fig. 12. 3-D CFD models air velocity profiles via [a] fabric duct at a medium level and [b] D-shape fabric duct at a medium level.

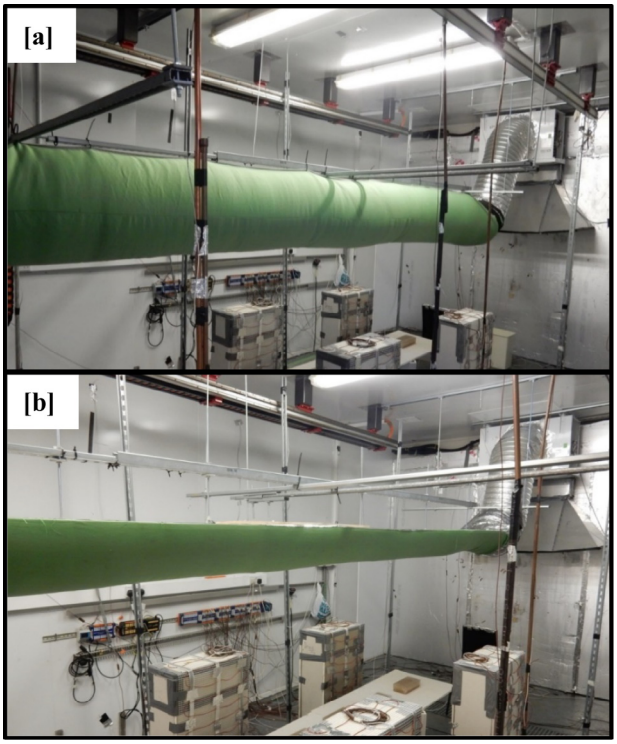

Fig. 13. Air distribution via [a] round fabric duct at a medium level and [b] D-shape fabric duct at a medium level.

stratification (of the order of 4 °C) takes place between head and ceiling level.

Fig. 15a and b show air velocities in the space for the round and D-shape ducts respectively installed at a medium level with a ±0.05 m·s^{-1} variation in each point of measurement. The highest values were measured at knee level and the lowest values at ceiling level. The very slow air movement at ceiling level maintained high temperatures in this region and created the temperature stratification that can be observed in Fig. 14.

The above experimental results confirm that air distribution via round and D-shape ducts installed at a medium level in the space can provide an appreciable temperature gradient along the height of the space when compared with ceiling mounted air supply systems. The fabric ducts located at medium level provide uniform cooling of the occupied zone rather than the whole space, which should result in energy savings.

3.4. Energy performance

The energy consumption of the refrigeration system that provided cooling to the room through each one of the investigated air distribution configurations (plain evaporator coil, round fabric duct at ceiling level, D-shape duct and round fabric duct at medium level) is presented in this sub-section. For each case, experimental data were collected for a week, however, since the condensing unit was in the open, the outdoor temperature was not under control. Therefore, it was selected a 17-h test period in which case the outdoor air temperature was around 8 °C. For clarity, power data measurements are presented for a period of one hour in Fig. 16. In addition, Table 4 summarises the average operating characteristics of the different systems, as well as the energy consumption results.

Each figure includes the power measurements for each system, including the energy consumption of the compressor, condenser fans, evaporator fan and control system. The fan speed of the evaporator was kept at its nominal value in the case of the air distribution via plain evaporator at ceiling level and round fabric duct at the ceiling and medium level.

The power consumption (P) of the refrigeration system with each configuration was then estimated by considering the sum of the instant power consumption of the refrigeration system during

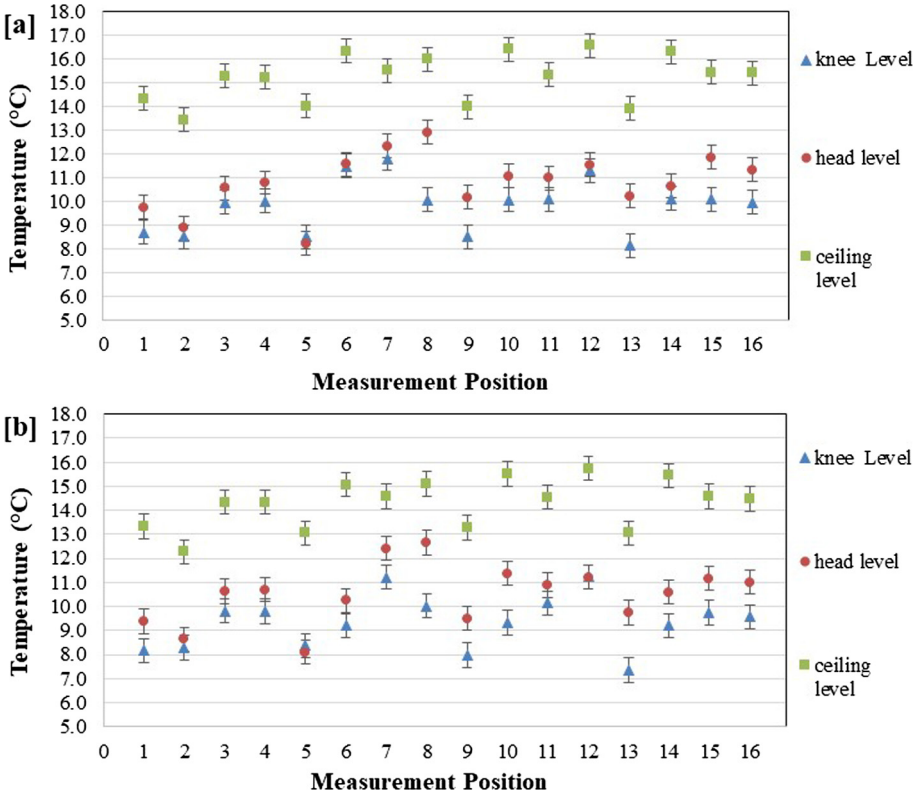

Fig. 14. Air temperatures profile for [a] round fabric duct at a medium level and [b] D-shape duct at a medium level.

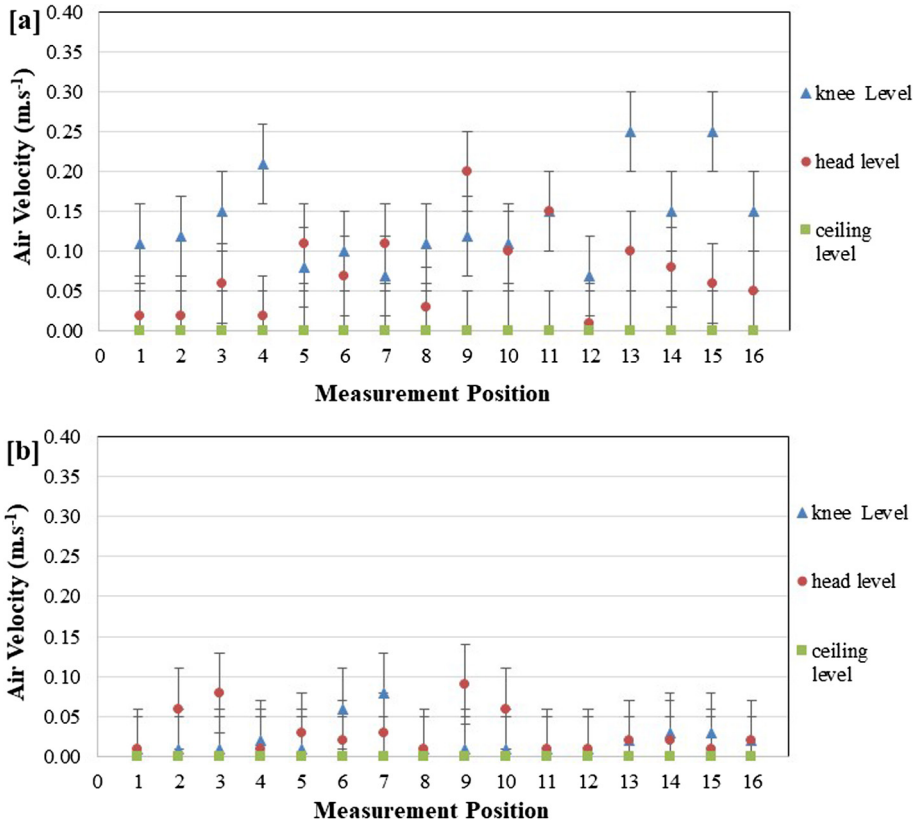

Fig. 15. Air velocity profile for [a] round fabric duct at medium level and [b] D-shape duct at medium level.

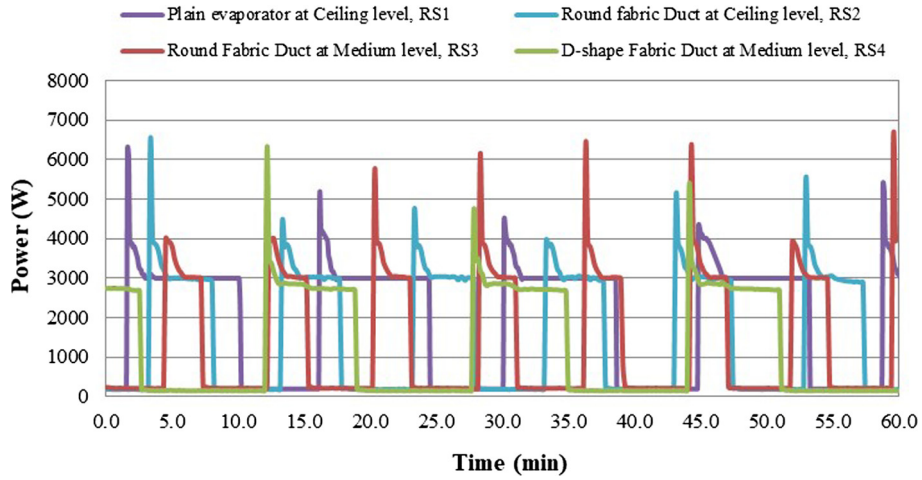

Fig. 16. Refrigeration system power consumption during a period of 1 h for Plain evaporator at Ceiling level, Round fabric Duct at Ceiling level, Round Fabric Duct at Medium level, and D-shape Fabric Duct at Medium level.

the running period (*P_on*) and the energy consumption of the condenser and evaporator fans and control system during the Stop period (*P_off*). Data collection occurred every 10 s.

$$P = \sum P\_on + \sum P\_off \tag{5}$$

Fig. 16 shows the power consumption of the refrigeration system with the air distribution via the non-ducted evaporator coil at ceiling level, referred to as Reference System 1 (RS1), whereas this figure also shows the power consumption of the refrigeration system with fabric duct air distribution at ceiling level which is referred to as Reference System 2 (RS1). The power consumption for air distribution via the round fabric duct (RS3) and D-shape fabric duct at a medium level (RS4) are also presented in Fig. 16.

A comparison of power consumption of the plain evaporator and round fabric duct at ceiling level depicts that the on-periods for the non-ducted evaporator coil are longer than those for the air distribution with the round fabric duct. This is primarily due to the high mixing of air in the space and lower temperatures without temperature stratification with the plain coil, as can be seen

Table 4
Operating characteristics and energy consumption of refrigeration system with the different air distribution methods.

Operating characteristics of the refrigeration system for a 17 h test period				
	Plain evaporator (Reference case 1)	Round fabric duct at High level (Reference case 2)	Round fabric duct at medium level with hood	D-shape fabric duct at medium level with hood
Total consumption (kWh)	30.05	25.28	22.88	23.51
Number of on/off cycles	71.40	102.00	122.40	57.80
Average 'on' time per cycle (in minutes)	7.60	4.26	3.00	7.80
Average 'off' time per cycle (in minutes)	6.10	5.70	5.40	9.80
Average instant power, on period (kW)	3.15	3.22	3.34	2.90
Average instant power, off period (kW)	0.20	0.20	0.22	0.17
Operating time per hour (in minutes)	31.92	25.56	21.60	26.52
Hourly average (kWh)	1.76	1.49	1.35	1.38
Energy saving (%)			Ref.1: 23%, Ref. 2: 9%	Ref. 1: 21%, Ref. 2: 7%

from Fig. 5, which requires the refrigeration system to run for a longer time to maintain on average a lower temperature in the space. These characteristics result in energy savings of 15% for the round fabric duct compared to the non-ducted evaporator coil.

Comparing the results of the round fabric duct at ceiling level and at a medium level, it can be seen that with the duct installed at a medium level, the on periods of the refrigeration system are shorter and the off periods longer. This is due to the fact that cooling is concentrated at a low level which reduces the area in the space that is cooled at low temperatures. From Table 4, the fabric duct at medium level results in energy demand reduction of 9% compared to ceiling mounted fabric duct and 23% energy demand reduction compared to the plain evaporator coil at ceiling level.

Regarding the energy consumption for the round duct and the D-shape duct installed at a medium level, as indicated in Section 3.1, the air flow with the D-shape duct was set at 70% of the air flow with the round duct to ensure similar air supply pressure to the room. Comparing the results in the two cases it can be seen that with the D-shape duct, the on-0off cycles of the refrigeration system are reduced significantly compared with the round duct. This is due to the lower flow rate in the space which also results in much lower velocities, as can be seen in Fig. 15, and slightly higher temperature stratification as shown in Fig. 14. From the results of Table 4 it can be seen that the D-shape duct results in energy demand reduction of the order of 7% compared to the round fabric duct at ceiling level and 21% over the plain evaporator coil at ceiling level.

Based on the power measurements and thermal environment obtained from each air distribution configuration, the feasibility of fabric ducts has been demonstrated, as they can be easily retrofitted onto existing air distribution systems and provide both energy savings and better thermal control conditions in the space through low air velocity supply and thermal stratification.

4. Conclusions

This paper details results of experimental investigations and CFD modelling aimed at improving the efficiency of air distribution and temperature control systems in chilled food manufacturing facilities. The investigations were carried out in a test chamber which was set up to simulate conditions in chilled food manufacturing facilities. These facilities normally have high ceilings and are served by non-ducted evaporator coils or diffusers located at ceiling level providing temperature control in the space through the mixing principle. These distribution systems invariably result in high velocities which lead to uncomfortable conditions for operators and energy wastage. A primary objective of the project was to demonstrate the feasibility of flexible systems that can be easily retrofitted onto existing air distribution systems and provide both energy savings and better thermal control conditions in the space through low air velocity supply and thermal stratification. Three alternative systems were investigated experimentally and by means of CFD models: a) air distribution through a round fabric duct at high level; ii) air distribution through a round fabric duct at medium level, and iii) air distribution through a D-shape fabric duct at medium level. The following conclusions can be drawn from the experimental and CFD modelling results:

- Experimental and CFD model results agreed that air distribution through fabric ducts result in lower air velocities and better thermal environments in chilled food manufacturing facilities compared to ceiling mounted non-ducted systems.
- Due to the low air discharge, velocities from the duct, even when mounted at ceiling level fabric ducts, develop a temperature stratification in the space. When the air entering the cooling coil is drawn from a lower level in the space, the system can lead to energy demand reduction and savings of the order of 15%, as demonstrated by the test results.
- Energy savings can increase further if the air is drawn from medium level, cooled in the coil and supplied at medium level just to cool the area in which food processing takes place. The results from medium level supply showed energy savings of the order of 23% over a non-ducted coil at ceiling level and 9% over a fabric duct distribution system mounted at ceiling level.
- Fabric duct air distribution systems are very flexible and easily adaptable for the cooling of large high ceiling places. An issue with their application in chilled food factories particularly when mounted at low level is the risk of wetting from cleaning the space on a daily basis. To address this issue, alternative materials of construction that can provide similar air distribution properties, but which can be easily cleanable, need to be identified.

Acknowledgements

This project was funded by Innovate UK and the RCUK Centre for Sustainable Energy Use in Food Chains through EPSRC grant No: EP/K011820/1. The authors acknowledge the support from Innovate UK, the RCUK energy programme and contributions from the industrial collaborators Bakkavor and Waterloo Air Products PLC.

Appendix A. Supplementary material

Supplementary data associated with this article can be found, in the online version, at http://dx.doi.org/10.1016/j.applthermaleng.2017.08.134.

References

[1] CFA, Climate Change Agreement - Chilled Food Sector Progress and Barriers, (2012). http://www.chilledfood.org/MEDIA/campaigns/Climate+Change+Agreement+-+Chilled+Food+Sector+Progress+and+Barriers.htm [Last access 02/03/17].

[2] Defra, Department of Environment, Food and Rural Affairs, Food Statistics Pocketbook, (2012) 86.

[3] S.J. Rees, P. Haves, An experimental study of air flow and temperature distribution in a room with displacement ventilation and a chilled ceiling, Build. Environment 59 (2013) 358–368.

[4] Y. Cheng, J. Niu, X. Liu, N. Gao, Experimental and numerical investigations on stratified air distribution systems with special configuration: thermal comfort and energy saving, Energy Build. 64 (2013) 154–161.

[5] Y.J.P. Lin, T.Y. Tsai, An experimental study on a full-scale indoor thermal environment using an Under-Floor Air Distribution system, Energy Build. 80 (2014) 321–330.

[6] A. Jurelionis, L. Gagyte, T. Prasauskas, Darius Ciuzas, E. Krugly, L Seduikyte, D Martuzevicius, impact of the air distribution method in ventilated rooms on the aerosol particle dispersion and removal: the experimental approach, Energy Build. 86 (2015) 305–313.

[7] K.-N. Rhee, M.-S. Shin, S.-H. Choi, Thermal uniformity in an open plan room with an active chilled beam system and conventional air distribution systems, Energy Build. 93 (2015) 236–248.

[8] N.J. Smale, J. Moureh, G. Cortella, A review of numerical models of airflow in refrigerated food applications, Int. J. Refrigerat. 29 (6) (2006) 911–930.

[9] A. Ambaw, M.A. Delele, T. Defraeye, Q.T. Ho, L.U. Opara, B.M. Nicolaï, P. Verboven, The use of CFD to characterize and design post-harvest storage facilities: Past, present and future, Comput. Electron. Agricult. 93 (2013) 184–194.

[10] O. Laguerre, S. Duret, H.-M. Hoang, L. Guillier, D. Flick, Simplified heat transfer modeling in a cold room filled with food products, J. of Food Eng. 149 (2014) 78–86.

[11] S. Duret, H.-M. Hoang, D. Flick, O. Laguerre, Experimental characterization of airflow, heat and mass transfer in a cold room filled with food products, Int. J. Refrigerat. 46 (2014) 17–25.

[12] M.A. Delele, A. Schenk, E. Tijskens, H. Ramon, B.M. Nicolaï, P. Verboven, Optimization of the humidification of cold stores by pressurized water atomizers based on a multiscale CFD model, J. of Food Eng. 91 (2) (2009) 228–239.

[13] M.A. Delele, M.E.K. Ngcobo, S.T. Getahun, L. Chen, U.L. Opara, Studying airflow and heat transfer characteristics of a horticultural produce packaging system using a 3-D CFD model Part I: Model development & validation, Postharvest Biol. Tech. 86 (2013) 536–545.

[14] M.K. Chourasia, T.K. Goswami, Simulation of effect of stack dimensions and stacking arrangement on cool-down characteristics of potato in a cold store by computational fluid dynamics, Biosys. Eng. 96 (4) (2007) 503–515.

[15] M.K. Chourasia, T.K. Goswami, Steady state CFD modeling of airflow, heat transfer and moisture loss in a commercial potato cold store, Int. J. Refrigerat. 30 (4) (2007) 672–689.

[16] M.K. Chourasia, T.K. Goswami, Three dimensional modeling on airflow, heat and mass transfer in partially impermeable enclosure containing agricultural produce during natural convective cooling, Energy Convers. Management 48 (7) (2007) 2136–2149.

[17] V. Chanteloup, P. Mirade, Computational fluid dynamics modelling of local mean age of air distribution in forced-ventilation food plants, J. of Food Engineering 90 (1) (2009) 90–103.

[18] S.H. Ho, L. Rosario, M.M. Rahman, Numerical simulation of temperature and velocity in a refrigerated warehouse, Int. J. of Refrigerat. 33 (5) (2010) 1015–1025.

[19] W. Pasut, F. Bauman, M. De Carli, The use of ducts to improve the control of supply air temperature rise in UFAD systems: CFD and lab study, Appl. Energy 134 (2014) 490–498.

[20] M.H. Fathollahzadeh, G. Heidarinejad, H. Pasdarshahri, Prediction of thermal comfort IAQ, and Energy consumption in a dense occupancy environment with the under floor air distribution system, Build. Environment 90 (2015) 96–104.

[21] K. Zhang, X. Zhang, S. Li, Simplified model for desired airflow rate in underfloor air distribution (UFAD) systems, Appl. Therm. Eng. 93 (2016) 244–250.

[22] M. Ning, S. Mengjie, C. Mingyin, P. Dongmei, D. Shiming, Computational fluid dynamics (CFD) modelling of air flow field, mean age of air and CO_2 distributions inside a bedroom with different heights of conditioned air supply outlet, Appl. Energy 164 (2016) 906–915.

[23] Y. Cheng, J. Niu, N. Gao, Stratified air distribution systems in a large lecture theatre: a numerical method to optimize thermal comfort and maximize energy saving, Energy Build. 55 (2012) 515–525.

[24] S.A.Tassou, B.L. Gowreesunker, D. Parpas, A. Raeisi. Modelling cold food chain processing and display environments, In Modelling Food Processing Operations. 185-208, Elsevier, April 2015, ISBN-139781782422846

[25] D.A. Parpas, C. Amaris, S.A. Tassou, B.L Gowreesunker, W. Terkuile, Investigation into air distribution systems and temperature control in chilled food manufacturing facilities, Sustainable Thermal Energy Management Network, 3rd Sustainable Thermal Energy Management Int. Conf., Newcastle upon Tyne, UK, 7-8 July, (2015) 110-119.

[26] Ke-fibertec KE - Low Impulse textile duct fabric. Available from: http://www.ke-fibertec.com/uk [Last access 02/03/17].

[27] Tsi airflow instruments Ltd. TSI TA465-P. Available from: http://www.tsi.com/airflow-instruments-multi-function-anemometer-ta465-p/ [Last access 02/03/17].

[28] Fluke, Fluke 435 Series II Power Quality and Energy Analyzer. Available at: http://en-us.fluke.com/products/power-quality-analyzers/fluke-435-ii-power-quality.html [Last access 02/03/17].

[29] Measuresoft datascan products and services (http://datascan.measuresoft.com/products/analog-modules/7020-16-channel-analog-input-module/) Datascan modules 7020 [Last access 02/03/17].

[30] ANSYS FLUENT Theory Guide, ANSYS, Inc. Release 14.0, Southpointe, 2011.

[31] A. Stamou, I. Katsiris, Verification of a CFD model for indoor airflow and heat transfer, Build. Environment 41 (2006) 1171–1181.

[32] F.R. Menter, Two-equation eddy-viscosity turbulence models for engineering applications, AIAA J 32 (1994) 1598–1605.

[33] ISO, Ergonomics of the thermal environment — Analytical determination and interpretation of thermal comfort using calculation of the PMV and PPD indices and local thermal comfort criteria, in: BS EN ISO 7730:2005.

[34] D. Parpas, C. Amaris, S.A. Tassou, Experimental study and modelling of air distribution systems and temperature control for chilled food factories in a scaled test facility, Proceedings of the 14th International Conference on Sustainable Energy Technologies, Nottingham, UK, 25 – 27 August, (2015), Volume II, pp 85-95. Available from: eprints.nottingham.ac.uk [Last access 02/03/17].